Journal of Atmospheric and Terrestrial Physics, Vol. 44, No. 5, pp. 425–440, 1982.
Printed in Great Britain.

0021 9169/82/050425-16 $03.00/0
Pergamon Press Ltd.

Departures from diffusive equilibrium in the topside F-layer from satellite soundings

M. LOCKWOOD* and J. E. TITHERIDGE

Radio Research Centre, The University of Auckland, Private Bag, Auckland, New Zealand

(*Received in final form* 12 *November* 1981)

Abstract—A method for the detection of O^+ ion fluxes from topside soundings is described. The shape of the plasma scale-height profile is altered by such flows only at heights near the $F2$-peak, where ion–neutral drag is large. Model profiles are used to relate changes in scale height to the ratio (ϕ/ϕ_L) where ϕ is the field-aligned O^+ flux (relative to the neutral air) and ϕ_L is the limiting value set by frictional drag. Values of (ϕ/ϕ_L) can then be determined to within a few per cent from experimental soundings, using the plasma temperature and its gradient (as deduced from the observed profile) and the MSIS model neutral temperature. It was found that 3700 topside profiles show departures from diffusive equilibrium, out of 10,000 used to obtain the global morphology of (ϕ/ϕ_L) near the sunspot minimum. Results reveal dynamic ion-flow effects such as the transequatorial breeze and the effects of the polar wind and protonospheric replenishment light-ion flows can be inferred.

1. INTRODUCTION

Field-aligned flows of ionization play an important role in the plasmasphere and upper ionosphere. Upward fluxes produce most of the ionization found at heights above 1000 km, while return flows are partly responsible for the maintenance of the night ionosphere. The flows consist primarily of O^+ ions near the peak of the $F2$-layer and H^+ ions at great heights. Incoherent scatter radars have been used to infer proton fluxes, at high altitudes, from the flux of O^+ ions observed closer to the $F2$-peak (e.g. EVANS and HOLT, 1978). Using the sensitive Arecibo radar, VICKREY *et al.* (1979) observed the field-aligned velocity components of both O^+ and H^+ ions and found them to be in opposite directions at certain times and altitudes. This 'counterstreaming' effect has been modelled by BAILEY *et al.* (1977a) using time-dependent equations of continuity and momentum for each ion species. YOUNG *et al.* (1980) showed that this effect also occurs under steady state conditions.

Incoherent scatter observations are restricted to a limited number of sounding locations. Satellite observations give global coverage; however *in situ* measurements yield information on flows only at the altitude of the satellite. The observed flux of any one ionic species, in the presence of others, will contain an unknown component due to differential flow patterns. Such effects are significant in a range of heights around the ion transition level (at which the densities of O^+ and H^+ are equal) so it is desirable to make observations of H^+ flows at altitudes well above this range. Similarly O^+ flows should be observed below this region, but at a height great enough to make photochemical effects negligible. The large variations in ion-transition height (TITHERIDGE, 1976a) make it impossible to select a satellite orbit for which this condition is always satisfied. Hence *in situ* observations of O^+ flows cannot be made such that the effects of charge exchange with H^+, recombination and production are all negligible at all times.

This paper presents a method of observing O^+ flows remotely from satellites using topside soundings. The altitude at which the measurement is made is chosen so that charge exchange and photochemical effects are minimized and changes in both the ion transition level and the $F2$-peak height are accommodated. The large amount of available data means that the method can be used to study the global morphology of departures from diffusive equilibrium in the topside F-layer. The flows are expressed as a fraction of their limiting value. The concept of a maximum flow rate, or 'limiting flux', was introduced by HANSON and PATTERSON (1964). Upward flows of light ions are restricted to this value by a diffusive barrier presented by Coulomb interaction with O^+ ions. The limiting light-ion flow was quantified by GEISLER (1967) for daytime conditions at middle latitudes. The result was assumed to set an upper limit to the size of return plasma flows from the protonosphere at night and hence to their contribution to the maintenance of the night F-region (RAITT and DORLING, 1976). It should be noted, however, that these calculations apply only to the movement of H^+ ions through O^+ ions; they do not place any restriction on overall flows in which both H^+ and O^+ ions move

* Present address: Rutherford Appleton Laboratory, Chilton, Oxon, OX11 0QX, U.K.

together (as in the diurnal 'breathing' of the ionosphere; TITHERIDGE, 1968).

An upward flow of H^+ ions, relative to the O^+ ions, is maintained by charge exchange between O^+ and H at lower heights (BANKS and HOLZER, 1969a). The flow of O^+ ions is limited by frictional drag with ambient neutral particles, in the same way that H^+ flux is limited by Coulomb drag with O^+. The restriction on the flow of H^+ through O^+ is commonly an order of magnitude smaller than that on the O^+ flowing through the neutral oxygen. Under steady state conditions the ion-flow at any altitude is restricted to the lower of the two limits and the O^+ flux is not generally close to its limiting value, set by frictional drag with the neutral gas.

2. LOW SPEED O^+ FLOW EQUATIONS

Ion-inertial effects can be neglected if the ion velocity, v, remains low enough to satisfy the inequality (BANKS and HOLZER, 1969a)

$$v^2 \ll kT_i/m_i, \tag{1}$$

where k is Boltzmann's constant and T_i and m_i are the O^+ ion temperature and mass respectively. The force balance equation along the geomagnetic field line for O^+ ions in an atmosphere of O atoms is then

$$-k \sin I\left(\frac{\mathrm{d}}{\mathrm{d}h}\right)(N_iT_i) - N_i m_i g \sin I + N_i eE = DN_iN_n(v_{il} - u_{il}), \tag{2}$$

where N_i and N_n are the densities of O^+ ions and O atoms respectively and v_{il} and u_{il} are their field-aligned velocities; I is the geomagnetic dip, h the altitude, E the electric field and D the frictional drag coefficient for O^+ ions moving through O. The equivalent equation for electrons is

$$-k \sin I\left(\frac{\mathrm{d}}{\mathrm{d}h}\right)(N_eT_e) - N_e eE = 0, \tag{3}$$

because the gravitational and drag terms are negligible for electrons; T_e is the electron temperature. The electron density, N_e, equals N_i at the altitudes close to the $F2$-peak which are considered here. The plasma scale height, H, is given by

$$H = -N_i\left(\frac{\mathrm{d}h}{\mathrm{d}N_i}\right). \tag{4}$$

The parameter ϕ is defined by

$$\phi = N_i(v_{il} - u_{il}). \tag{5}$$

Hence ϕ is the field-aligned flux of O^+ ions, relative to the neutral atmosphere. Note that ϕ differs from (N_iv_{il}), which is the definition of flux usually adopted, as for example in studies using incoherent scatter radars. Adding equations (2) and (3) and substituting (4) and (5) gives

$$\phi = \left\{\frac{N_i}{N_n}\right\}\cdot\frac{\sin I}{D}\left\{\frac{H_0}{H} - 1\right\}\cdot\left\{k\left(\frac{\mathrm{d}T_t}{\mathrm{d}h}\right) + m_i g\right\}, \tag{6}$$

where T_t equals $(T_e + T_i)$. H_0 is the value of H when ϕ is zero, hence it is the diffusive equilibrium scale height and is given by

$$H_0 = \left\{\frac{m_i g}{kT_t} + \frac{1}{T_t}\left(\frac{\mathrm{d}T_t}{\mathrm{d}h}\right)\right\}^{-1}. \tag{7}$$

Under limiting flux conditions ($\phi = \phi_L$) the plasma density decreases with the scale height of the friction-producing medium—in this case H_n, the scale height of the neutral oxygen atom gas (BANKS and HOLZER, 1969a). Neglecting the small variation of D with ϕ (BANKS and HOLZER, 1969b) equation (6) yields

$$(\phi/\phi_L) = \left\{\frac{N_i}{N_{iL}}\right\}\left\{\frac{H_0/H - 1}{H_0/H_n - 1}\right\}, \tag{8}$$

where N_{iL} is the plasma density under limiting flux conditions. Figure 1 shows an example set of plasma density profiles, modelled for various values of ϕ using the model of TITHERIDGE (1976a). If the extrapolations of topside profiles for fluxes [as defined by equation (5)] of ϕ and ϕ_L intersect at a reference height h_1 (as shown in Fig. 1), then equation (8) can be re-written

$$(\phi/\phi_L) = \frac{\Delta T_n}{H(T_t - T_n)}\exp\left\{(h_d - h_1)\left(\frac{1}{H_n} - \frac{1}{H}\right)\right\}, \tag{9}$$

where Δ is $(H_0 - H)$ at the height h_d (see Section 4) and T_n is the neutral temperature. The assumption that ion-inertial effects can be neglected is investigated in Appendix B.

3. ANALYSIS OF TOPSIDE SOUNDINGS

Topside electron-density profiles (60,000 in total) have been calculated at the Communications Research Centre, Ottawa, from ionograms obtained between 1962 and 1968 by the *Alouette 1* satellite. Consecutive profiles were corrected for horizontal gradients and averaged in groups of about six to obtain mean field-aligned variations (as described in TITHERIDGE, 1976a). This yielded 10,000 profiles of plasma scale height H, defined by equation (4), at altitudes of about 400–1000 km. An example of one such profile is given by the points in Fig. 2 (a). The curve (b) is the best-fitting diffusive equilibrium profile H_p produced using the model of TITHERIDGE (1976a). The fit was obtained by varying the plasma temperature, temperature gradient

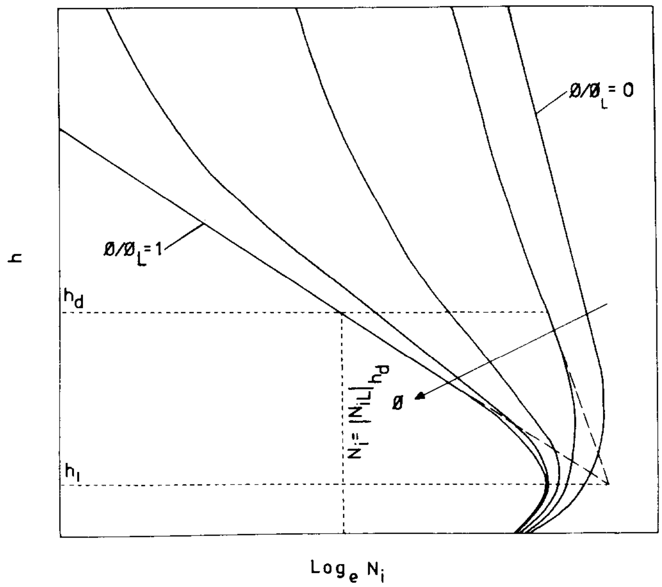

Fig. 1. Example set of model scale-height profiles for ϕ ranging between zero and ϕ_L; h_1 and h_d are the reference and scaling heights (see Sections 2 and 3 of text, respectively).

and ion composition inputs to the model. The presence of any vertical H^+ flux is effectively allowed for by the composition adjustment, which alters the O^+/H^+ transition height. However, the curve H_p does not include the effect of any O^+ flux. It also omits F-layer production and loss processes; hence H_p does not become infinite at the $F2$-peak and it is not fitted to values of H below 400 km.

In most cases the agreement between H and H_p is considerably closer than in Fig. 2. The example shown

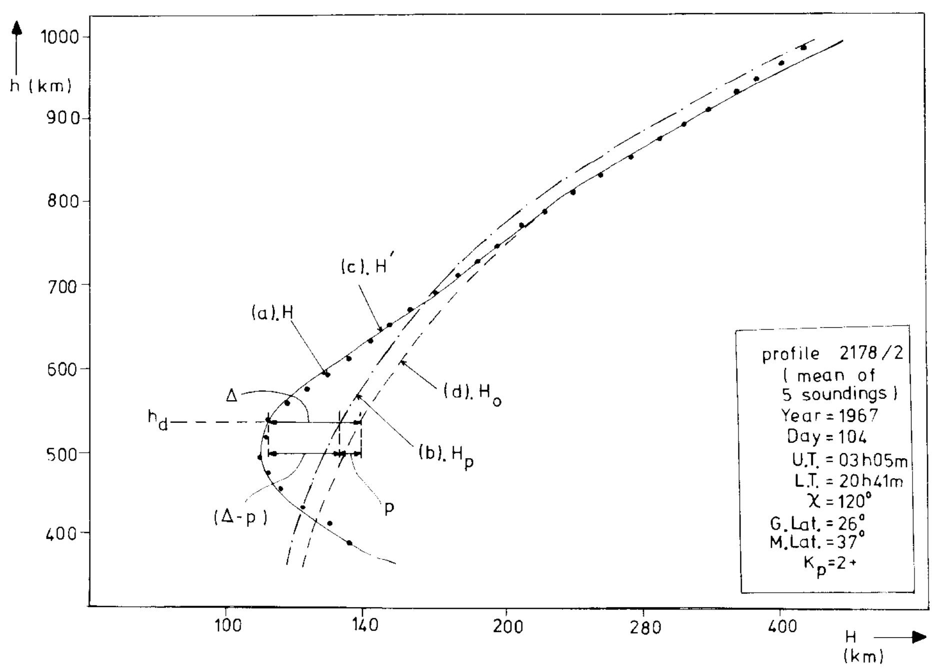

Fig. 2. Example set of plasma scale-height profiles: (a) H, the observed profile; (b) H_p, best-fit, diffusive equilibrium model profile; (c) H', full modelled profile; and (d) H_0, diffusive equilibrium profile for conditions of (c). Δ and p are scaled off at the height h_d.

does, however, illustrate an effect which is observed in 37% of all cases. The observed scale height H is consistently less than H_p at altitudes just above the $F2$-peak. The decrease occurs in the 400–700 km altitude range and can be modelled by including the effect of field-aligned O^+ flows. This flow affects the scale-height profile only in the lower topside ionosphere, where ion-neutral drag is important. This can be seen in equation (6); when the concentration of the friction-producing gas, N_n, is large then an upflux of ions ($\phi > 0$) causes H to be less than the value H_0 for diffusive equilibrium ($\phi = 0$). At greater altitudes the ionized fraction (N_i/N_n) becomes very large and H approaches H_0, independent of the value of ϕ.

The curve (c) in Fig. 2 was produced by modelling the profile separately in the 400–700 and 700–1000 km ranges, and ensuring continuity across the 700 km level. In the lower range production and loss effects were included but H^+ ions neglected, whereas in the upper range H^+ ions were included but there was no production or loss. The values of plasma temperature, temperature gradient, O^+ flux and ion composition were iterated starting from the values used to produce curve (b). Reasonable agreement at all altitudes was eventually achieved, as shown in Fig. 2 (c). The curve (d) in Fig. 2 is the diffusive equilibrium profile (neglecting peak effects) for the composition and temperature values used in (c). Calculation of the best least-square fit (c) determines the magnitude of the O^+ flux to within a few per cent. The computer time required is, however, too long for processing of 10,000 profiles. Plots of the data (a) and the best-fit diffusive equilibrium model (b) were available for each profile (from the work of Titheridge, 1976a). Model calculations were therefore used to calibrate the maximum displacement of the smoothed curves in the region of interest ($\Delta - p$, Fig. 2) to give a direct measure of flux effects.

4. CALCULATION OF THE O^+ FLUX

4.1. *Measurement and calibration of the scale-height changes*

The 10,000 plotted profiles were sorted manually and 3700 were selected for which H deviated from H_p in the manner illustrated by Fig. 2, and by an amount which exceeded the combined errors in H and H_p. From each pair of observed and best-fit (diffusive equilibrium) profiles the quantity ($H_p - H$) was measured, at a height h_d chosen to be just above the peak deviation of H from H_p. Below this altitude the production and loss terms become important and the theory outlined in Section 2 cannot be applied. Above h_d the deviation of H from H_p

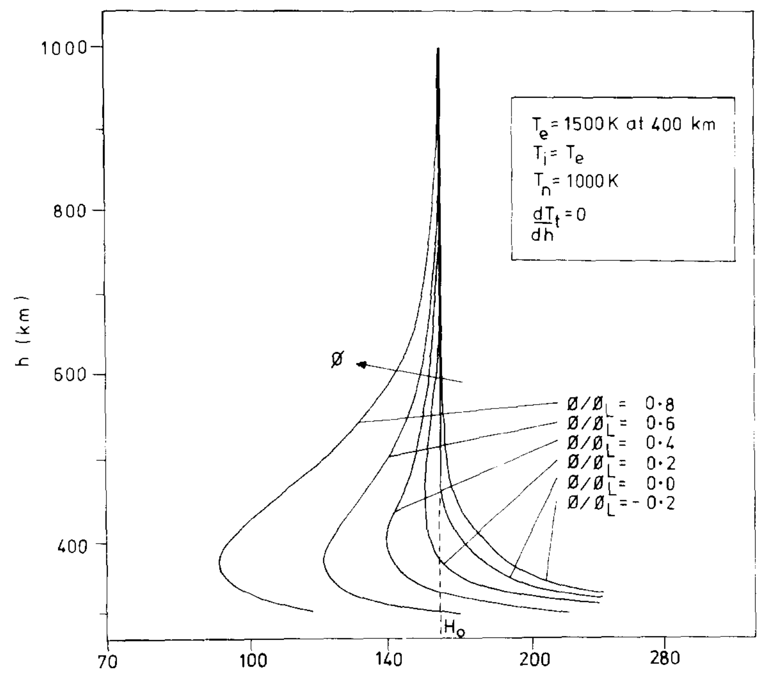

Fig. 3. Model scale-height profiles for a pure O^+ ionosphere, with the ion-flow ϕ equal to various fractions of the limiting value ϕ_L. The neutral temperature is 1000 K and the plasma temperature is 1500 K at all altitudes; ($T_t = T_e + T_i$).

is reduced by the decreased neutral density and hence measurement sensitivity is lost. If H_p is shifted from H_0 by an amount p at the height h_d, where H deviates from H_0 by Δ (Fig. 2), then

$$[H_p - H]_{h=h_d} = (\Delta - p). \quad (10)$$

The plasma scale-height profile of an ionosphere containing only O^+ ions was modelled numerically for a variety of steady state conditions. For given profiles of plasma temperature, neutral temperature, production and loss rates, a model was produced by integrating upwards in small steps from an initial plasma density value below the $F2$-peak. Reducing this initial density has the effect of increasing the upward ion flux ϕ in the topside ionosphere (as in Fig. 1). The initial plasma density could therefore be iterated until certain conditions were met. Results were obtained for diffusive equilibrium ($\phi = 0$) and for the limiting flux ($\phi = \phi_L$). This latter condition is indicated by the plasma density decreasing with the same scale height as the friction-producing, neutral atmosphere. Finally fluxes equal to various fractions of ϕ_L were achieved. Figure 3 shows a set of profiles produced in this way for zero plasma temperature gradient and Fig. 4 is a similar set for a gradient of 0.9 K km^{-1}.

Each model scale-height profile was fitted with a diffusive equilibrium profile, H_p, using the same procedure that was used to fit the experimental data. In this way Δ and p were calibrated over the range of conditions expected in the topside ionosphere. Figure 5 shows calibration curves of $(\Delta - p)$ as a function of (ϕ/ϕ_L) for various values of the plasma temperature, $(T_t/2)$. In this example the neutral temperature T_n is equal to 1000 K and the ion fluxes are upward. For values of (ϕ/ϕ_L) less than approximately 0.7 the curves can be expressed as a polynomial in $(\Delta - p)$ multiplied by a function of H_0

$$(\phi/\phi_L)_m = f[(\Delta - p)F(H_0)]. \quad (11)$$

The subscript m is used to emphasize that this value is based on the model conditions used to generate Fig. 5. The effects of variations in these conditions must now be included. In addition only H and H_p can be measured from the plotted data and H_0 is generally unknown.

4.2. *Effects of temperature gradients*

The neutral temperature at the height h_d is close to its constant, exospheric value. Neutral temperature gradients are therefore neglected. Comparison of Figs 3 and 4 shows, however, that positive plasma temperature gradients of the order of magnitude observed in the topside ionosphere (TITHERIDGE, 1976b) cause variations in $(\Delta - p)$, especially in quasi-diffusive equilibrium cases. This effect is allowed for by

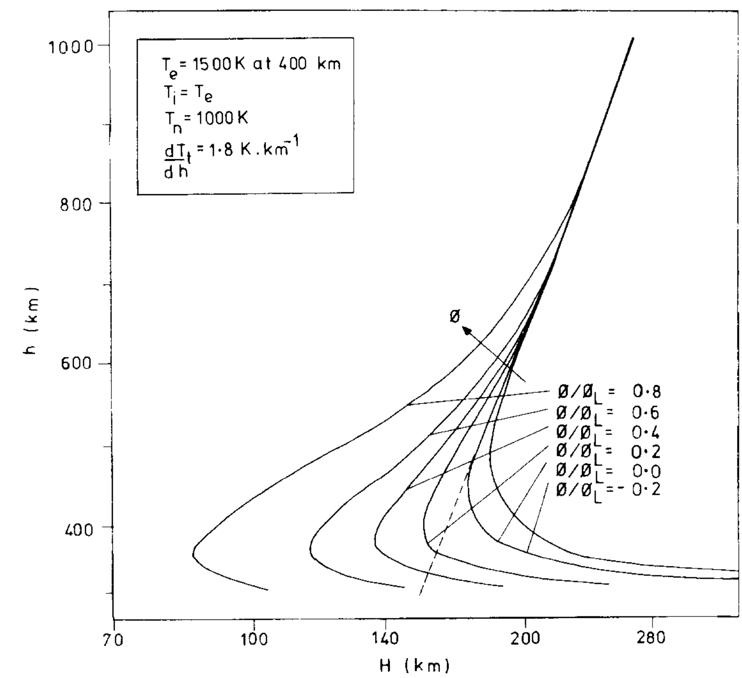

Fig. 4. Model scale-height profiles (see Fig. 3) for a plasma temperature of 1500 K at 400 km and a plasma temperature gradient of 0.9 K km^{-1} at all altitudes.

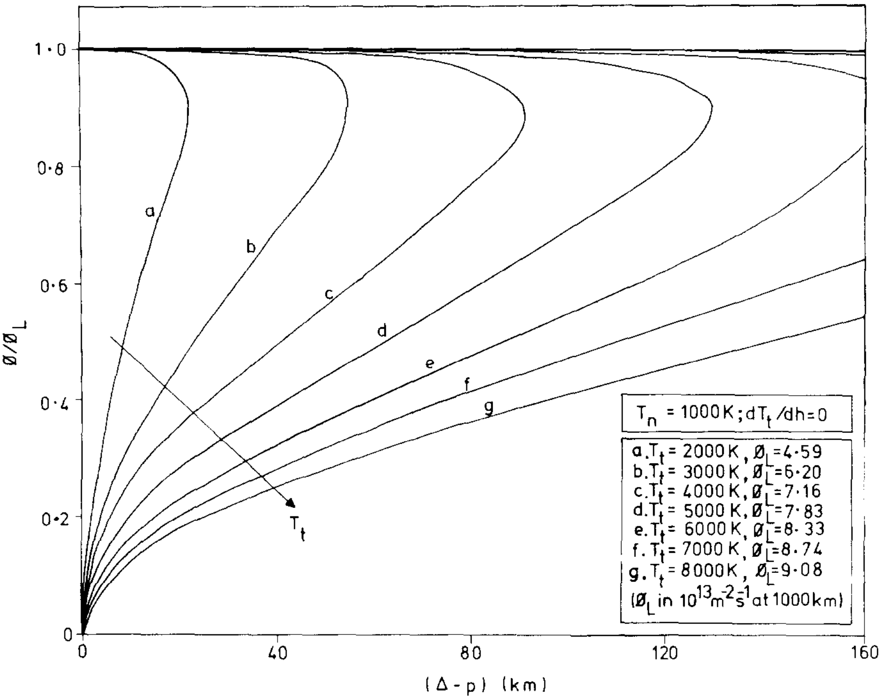

Fig. 5. Calibration curves of $(\Delta - p)$ as a function of (ϕ/ϕ_L), for various plasma temperatures. The neutral temperature is 1000 K and the plasma temperature gradient is zero.

using a correction factor

$$R = [(\Delta - p)F(H_0)]_{G=0}/[(\Delta - p)F(H_p)]_G, \qquad (12)$$

where G is the plasma temperature gradient as deduced from the best-fit profile H_p. This definition of R removes the requirement to evaluate H_0 and $(\mathrm{d}T_t/\mathrm{d}h)$. A calculated set of curves for R is shown in Fig. 6, as a function of a product of parameters which can all be scaled from the $H(h) - H_p(h)$ profile pair. This product is zero for diffusive equilibrium and ϕ equals ϕ_L at all points along the dashed curve. R falls from unity at large values of (ϕ/ϕ_L) due to the deviation of H_p from H_0; it also decreases near diffusive equilibrium due to the dependence of $(\Delta - p)$ on the plasma temperature gradient. Calibration curves of this type, giving R in terms of $\Delta - p$ and G, were produced for various values of H_p. The value of R for any required conditions could then be obtained by linear interpolation.

4.3. *Effect of neutral temperature*

Equation (9) shows that the other major parameter for which the value of (ϕ/ϕ_L) must be corrected is the neutral temperature, T_n. The dependence on other variables, for example the neutral density, is removed by expressing the flux as a ratio of its limiting value. By neglecting plasma temperature gradients equation (9) gives a first order correction to the value of (ϕ/ϕ_L), given by equation (11), as

$$(\phi/\phi_L) = (\phi/\phi_L)_m \left\{\frac{(T_t/1000) - 1}{(T_t/T_n) - 1}\right\} \times \exp\left\{\frac{mg(h_a - h_1)}{k}\left(\frac{1}{T_n} - \frac{1}{1000}\right)\right\}. \qquad (13)$$

The value of $(h_a - h_1)$ is approximately constant and is set equal to the value for $T_n = 1000$ K. The correction factor in equation (13) then rarely exceeds 10% and should be accurate to within a few per cent.

4.4. *Effect of the direction of flow*

Upward O^+ ion fluxes reach a maximum value at an altitude between the $F2$-peak and the ion-transition height (EVANS, 1975). Due to loss reactions in the F-region the flow decreases with decreasing altitude and is downward near the $F2$-peak. At greater altitudes O^+ is converted into H^+ by the charge exchange reaction. When the flows are upward the ion transition height is raised (TITHERIDGE, 1976a) and it is possible to find altitudes where the O^+ flux is not reduced by either effect and hence, by continuity, equals the total ion outflow from the ionosphere (under steady state conditions; EVANS and HOLT, 1978). At mid-latitudes the flux is often downward at night (RAITT and DORLING, 1976), which lowers the ion transition height

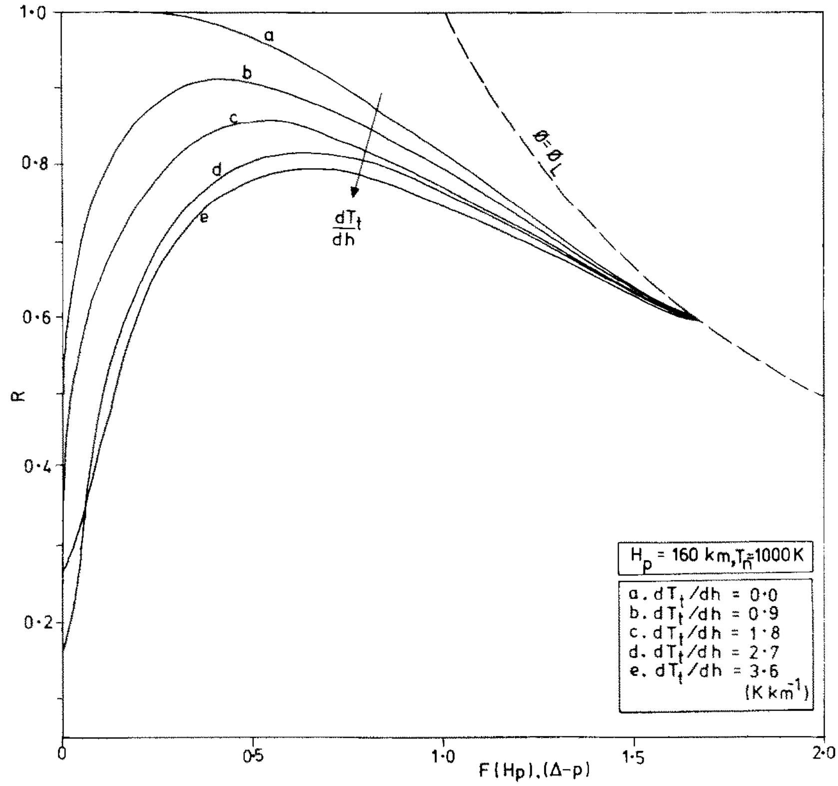

Fig. 6. Calibration curves of the R factor (see text) for various plasma temperature gradients.

at a time when the $F2$-peak is raised. Then there may not be an altitude at which the above conditions are met and the O^+ flux is a poor indicator of the ionosphere–protonosphere coupling flow (BAILEY *et al.*, 1977b).

Figure 7 shows three examples of $H(h) - H_p(h)$ profile pairs in the general case when both O^+ and H^+ ions are present. In the case of upward flows ($\phi/\phi_L > 0$), h_d and $(\Delta - p)$ are independent of the ion transition height h_T. For downward flows ($\phi/\phi_L < 0$), h_d increases and $(\Delta - p)$ decreases with higher values of h_T. As is demonstrated by Fig. 7, the effect of the profile fitting procedure is such that flows in either direction give positive values of $(\Delta - p)$, as defined by equation (10) and the sense of flow must be determined from the value of h_d. It is, however, difficult to devise an algorithm which can determine the sense of flow for all cases. Hence for the initial results presented in Section 5 the global morphology of the modulus of (ϕ/ϕ_L) is studied, to define those areas where large departures from diffusive equilibrium occur. For later, more detailed studies of these regions h_d will be used to determine the sense of flow. When flows are downward the calibration procedure is valid for only one value of h_T. Variations of h_T between 600 and 800 km introduce additional errors in (ϕ/ϕ_L) of up to 20% in the range $0 > \phi/\phi_L > -0.7$. In most cases the downward flow is underestimated, because $(\Delta - p)$ decreases with h_T.

4.5. *Analysis procedure and overall accuracy*

Values of $(\Delta - p)$, H_p and G are read off from each $H(h) - H_p(h)$ profile pair, and the corresponding value of R is interpolated. From equations (11) and (12) a value of $(\phi/\phi_L)_m$ is calculated, to which the correction given by equation (13) is applied using the neutral temperature derived from the MSIS model (HEDIN *et al.*, 1977). Use of this mean model for T_n introduces an error of up to a few per cent into each value of (ϕ/ϕ_L). Averaging sufficient numbers of observations should reduce this error.

The entire procedure was tested by applying it to model profiles of the type shown in Figs 3 and 4 for which the (ϕ/ϕ_L) values are known. These tests were carried out for various permutations of the model input data. In every case the deduced value of (ϕ/ϕ_L) was found to differ from the true value by an amount which was smaller than the error which would be caused by the experimental uncertainty in $H(h_d)$. The errors were typically a few per cent and hence comparable to those

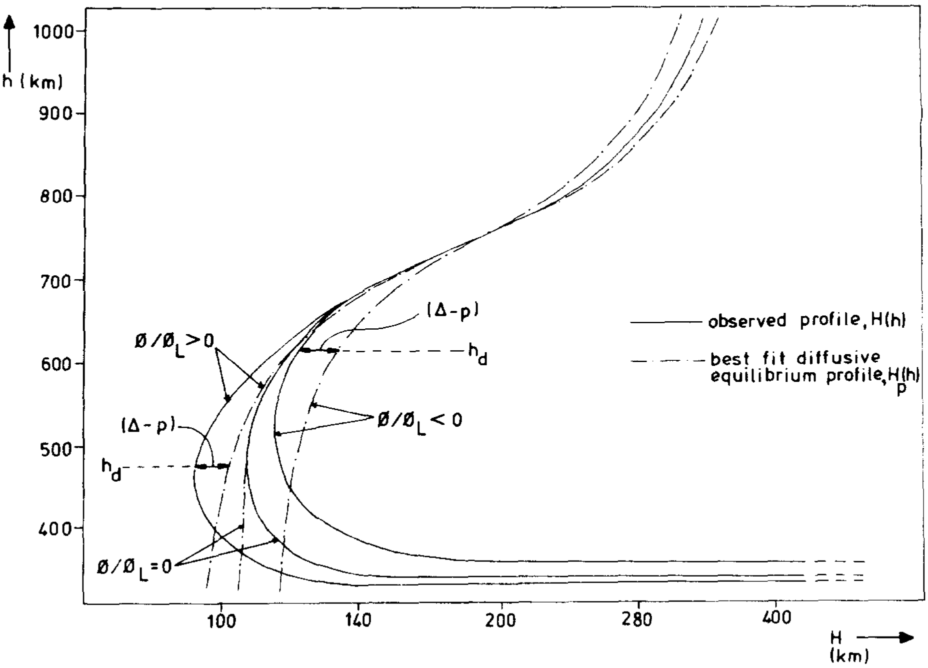

Fig. 7. $H(h)-H_p(h)$ profile pairs for upward, downward and zero O^+ fluxes when the ion transition level is low.

introduced by the use of a mean model for T_n. Individual values of the ratio (ϕ/ϕ_L) should therefore be accurate to within about ± 0.03. The mean values presented in Figs 8–12 have standard errors of a similar amount, in general, due to the spread of individual results. These means include the cases for which there was no measurable O^+ flux effect in the scale-height profile so that $(\phi/\phi_L)=0$.

5. RESULTS AND DISCUSSION

5.1. *Overall variations*

All observations of (ϕ/ϕ_L), for 100-day periods centred on the solstices and equinoxes, were used to obtain the mean variations in Fig. 8. The points plotted are averages over all local times and in 5° bins of geomagnetic latitude. In all seasons the lowest values are at auroral and sub-auroral latitudes. Equatorward of this minimum the mean values are highest in summer and lowest in winter; near the poles they are comparable for summer and the equinoxes, but larger during winter by a factor of two.

Smoothed latitudinal variations are shown in Figs 9 and 10, at intervals of 2 h LT. The mean values are for all observations taken within 50 days of the December solstices. Figure 9 gives results for the northern hemisphere, and Fig. 10 for the southern (where insufficient data was obtained at latitudes below −70° due to the lack of telemetry stations). The total number of profiles used in these two figures is 2786, each profile being the mean of about six observations. Averaging over local time ranges 4 h long and 2 h apart and geomagnetic latitude bins 10° wide and 5° apart, gives an average of 25 samples/bin. The averaging is performed over all universal times and K_p and over a 100-day period, so there is much variation within each mean and between adjacent bins.

Some of the larger-scale features of topside *F*-region dynamics at various latitudes can be seen in these plots and are discussed below. Appendix A considers the factors which influence (ϕ/ϕ_L). Equation (A7) shows that ϕ, as defined by equation (5), depends only on the ion concentration, the orientation of the geomagnetic field and the velocity due to diffusion. Thermospheric winds do not affect ϕ directly, but only by re-distributing plasma and hence altering the diffusion velocity.

5.2. *Low latitudes*

In all seasons the largest departures from diffusive equilibrium occur at equatorial latitudes. The solid dots in Fig. 8(a) mark the highest latitudes for which the magnetic field line lies beneath the mean O^+/H^+ ion transition height (as determined from this data set, TITHERIDGE, 1976a) at all points in that hemisphere. At lower latitudes O^+ is the dominant ion at all points

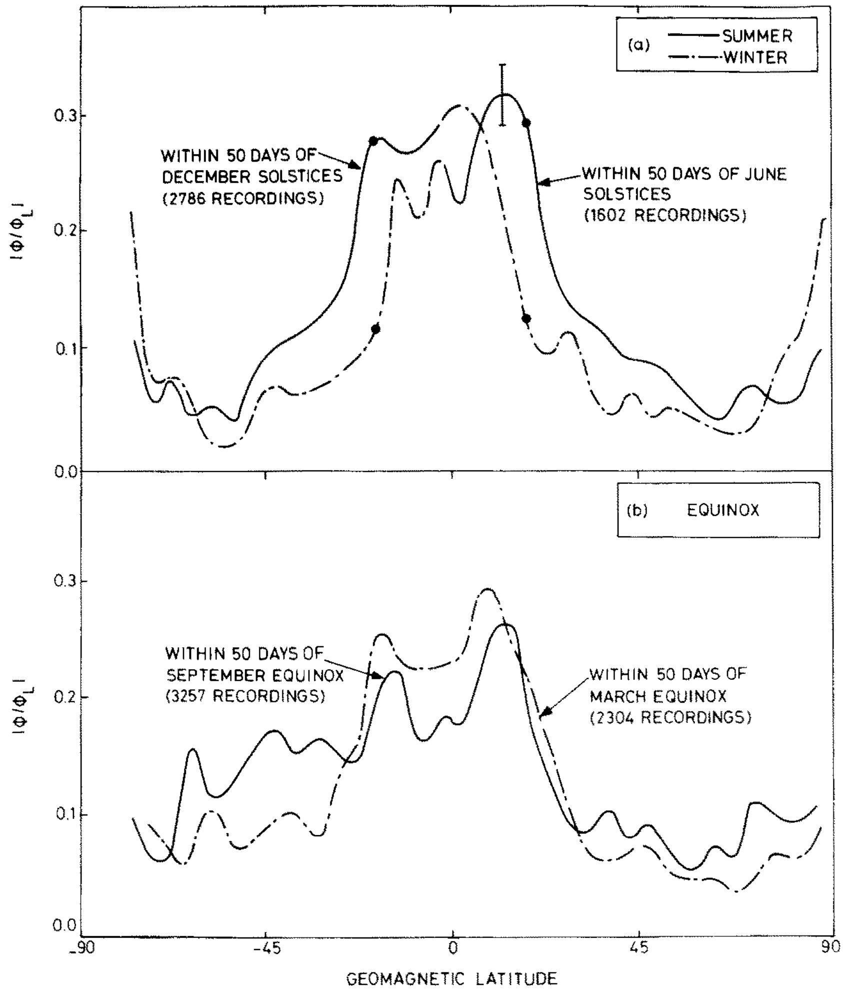

Fig. 8. Means of $|\phi/\phi_L|$ as a function of geomagnetic latitude, for summer and winter observations (a) and for equinox (b). Between the large dots in (a), O^+ is the dominant ion at all points along the field lines.

along the field lines. O^+ densities are also increased, by the equatorial 'fountain' effect, and large inter-hemispheric flows arise from the difference between the plasma pressures in the conjugate $F2$-regions (BAILEY and MOFFETT, 1979). The O^+ pressure difference between the feet of the field lines is largely due to the neutral thermospheric wind (RISHBETH, 1977) and causes a plasma flux from the summer to the winter hemisphere of the order of 2×10^{13} m^{-2} s^{-1} (BAILEY and MOFFETT, 1979). This transequatorial 'breeze' has been inferred from retarding potential analyser data from AE-C (HEELIS *et al.*, 1978) and OGO 6 (RISHBETH *et al.*, 1977). The mean diurnal variation in $|\phi/\phi_L|$ for the 10–30° geomagnetic latitude range (Fig. 11a, Section 5.4) shows a sharp minimum at 06.00 LT when plasma densities are small in both hemispheres. Near 14.00 LT, $|\phi|$ consistently exceeds $0.5\phi_L$ at latitudes of less than 20° (Figs 9 and 10).

There are some problems in the interpretation of the equatorial data, due to horizontal gradients of plasma density associated with the equatorial anomaly. In order to obtain the field-aligned scale height, H, a correction is made to the observed vertical value, H_v, for the horizontal scale height in the north–south direction, H_x (TITHERIDGE, 1976a). The value of H_x used at all altitudes is that observed along the orbital path of the satellite. At most latitudes any variation of H_x with altitude causes no significant error in the value of (ϕ/ϕ_L), since the correction is negligible at the height h_d (TITHERIDGE, 1976a). The correction is, however, proportional to $(H_v/H_x \tan I)$. Hence when the magnetic dip (I) is small the correction becomes very

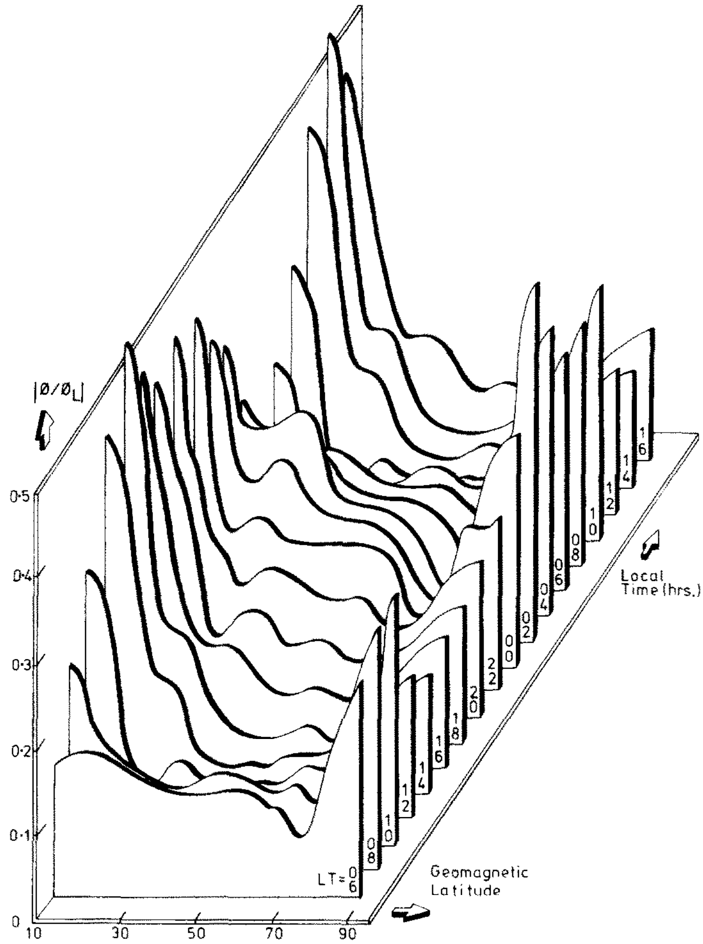

Fig. 9. Winter, northern hemisphere. The variation of mean $|\phi/\phi_L|$ with latitude and with local time, for all observations taken within 50 days of the December solstices.

large and the decrease of H_x with height due to the geomagnetic anomaly is a potential source of error at latitudes below about 10°. In addition the approximation employed in Appendix A breaks down at these latitudes and consequently the large field-aligned wind component may have some effect on (ϕ/ϕ_L). These effects are negligible at latitudes greater than about 10°.

5.3. *Mid-latitudes*

Field-aligned O^+ fluxes decrease rapidly at geomagnetic latitudes greater than about 20°, in Fig. 8. This agrees with the approximate limit of the equatorial 'fountain' effect (e.g. RISHBETH, 1977). At higher latitudes the field lines enter the protonosphere, which acts as a reservoir with variable H^+ content and prevents direct coupling between the conjugate *F*2-layers (BAILEY *et al.*, 1978). The reduction of diffusive flow at the boundary of the equatorial and mid-latitude ionospheres has been invoked to explain the variation of TEC observations in the vicinity of the equatorial anomaly (RAJARAM, 1977). For latitudes of 30–50° the mean flux ratio is about 0.06 in winter and 0.10 in summer for both hemispheres. Mean equinox values are about 0.085 for the northern hemisphere, but increases to 0.16 near the September equinox in the southern hemisphere.

Various numerical models have been used to aid understanding of plasma interchange between the ionosphere and magnetosphere within the plasmapause (e.g. MURPHY *et al.*, 1976; MARUBASHI, 1979; YOUNG *et al.*, 1980). Incoherent scatter observations at Arecibo by VICKREY *et al.* (1979) on one summer and one winter day showed that flows were upward during the day for both ion species at all heights in the topside ionosphere. This daytime refilling of the protonosphere is reproduced by all models. At night the fluxes were

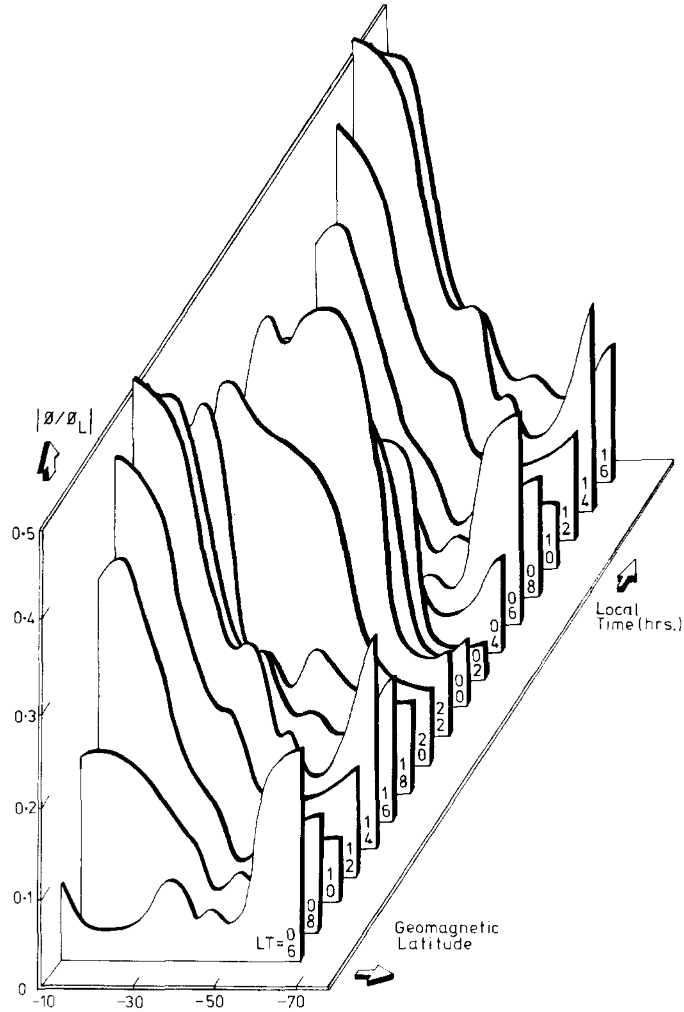

Fig. 10. Summer, southern hemisphere. The variation of mean $|\phi/\phi_L|$ with latitude and with local time, for all observations taken within 50 days of the December solstices.

downward before midnight and then briefly before dawn. This behaviour at inner plasmaspheric latitudes ($L = 1.4$) is reproduced by the model of MURPHY *et al.* (1976). Closer to the plasmapause the protonosphere is constantly in a state of recovery from depletion during geomagnetic storms, hence upward fluxes are expected to persist for most of the night (MARUBASHI, 1979). The incoherent scatter observations available at $L = 3.2$ (EVANS and HOLT, 1978) measure O^+ flows only and the nocturnal plasmasphere–ionosphere interchange flux is difficult to detect, as was discussed in Section 4.4.

5.4. *Storm effects*

Mean values of $|\phi/\phi_L|$ were determined at 3 h intervals of local time using data from all seasons and over a latitude range of 20°. Observations taken within 12 days following a storm sudden commencement (with $K_p > 4+$ on the following day) were excluded. Results for low- and mid-latitude ranges are shown by the dashed curves in Figs 11(a) and 11(b) respectively. Vertical bars show the standard errors of the calculated mean values.

For the 10–30° geomagnetic latitude range, smallest values of $|\phi/\phi_L|$ are found near dawn. At this time the equatorial F-layer is severely depleted due to the lack of maintaining flows from the protonosphere (RISHBETH, 1977). The solid line in Fig. 11(a) indicates the variation when D_a, the number of whole days following a storm sudden commencement, is less than 12. Results are given only where sufficient observations are available. Departures from diffusive equilibrium are much larger following a sudden commencement, returning to quiet-

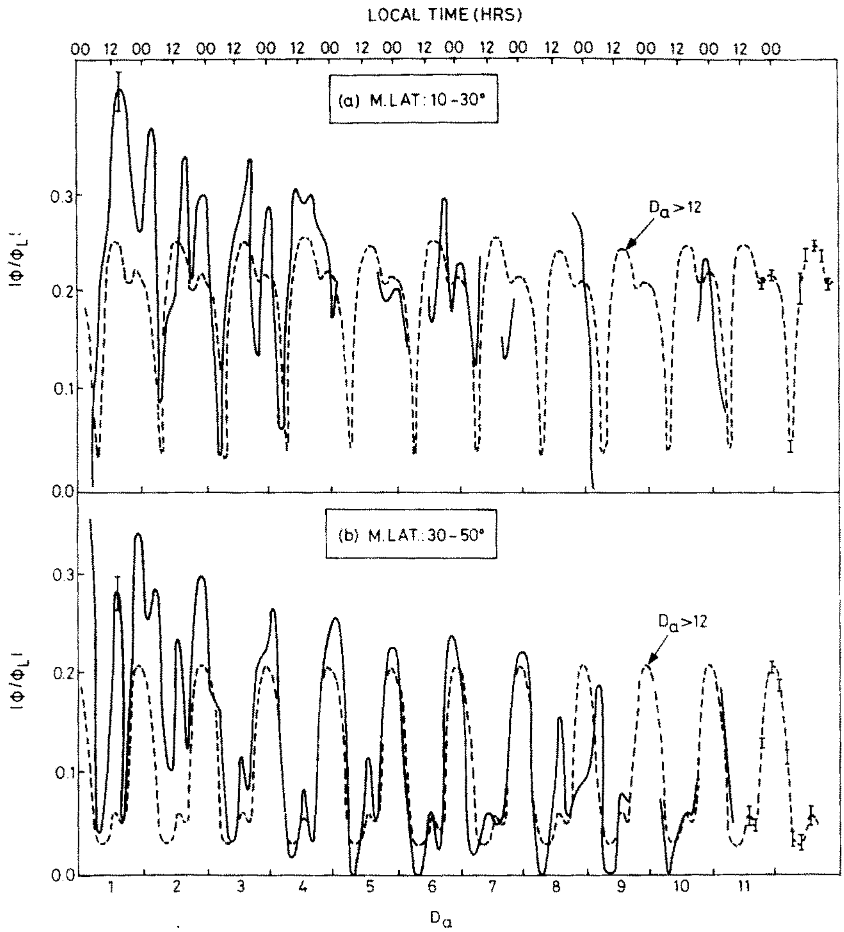

Fig. 11. Mean values of $|\phi/\phi_L|$ as a function of local time for low (a) and middle (b) latitude ranges. The solid curves are for various D_a, the number of days following a storm sudden commencement. Dashed curves show the variation for D_a greater than 12.

time values in about 4 days. The minimum near dawn is seen at all activities.

Figure 11(b) gives corresponding results for the 30–50° geomagnetic latitude range. The largest values of $|\phi/\phi_L|$ are found for quiet-times ($D_a > 12$) before midnight. This corresponds to a peak in the mean value of h_d indicating that these flows are often downward. Results show again that following a storm, departures from diffusive equilibrium are considerably increased.

The enhanced convection electric field pushes plasma down into the ionosphere on the nightside during the onset of a storm. On the dayside it 'peels' plasma off. Both processes deplete the plasmasphere, especially at the higher latitudes. In response, enhanced replenishment, supported by O^+ fluxes via charge exchange, is expected. From whistler data Park (1974) found that at $L = 3$ this refilling persisted for 3 days following a storm. The model of Murphy *et al.* (1976) for sunspot minimum indicates that a figure of 8 days may be more appropriate. Figure 11(b) shows that O^+ flux ratios are enhanced for about 7 days following storms, a figure consistent with the findings of Park (1974) for the outer plasmasphere at $L = 4$. The minimum flux is close to zero from day 5 to about day 10, following the storm sudden commencement.

5.5. *High latitudes*

Within the polar cap h_d rarely exceeds the height of the $F2$-peak by more than 200 km. Hence observed departures from diffusive equilibrium are nearly always due to upward flows (Section 4.4). Such upward fluxes are expected at these latitudes, as they are required to support the light ion polar wind outflow at greater heights (Banks and Holzer, 1969a,b). The roll-modulation of results from the ISIS 2 ion mass spectrometer show the polar wind to be predominantly protons as predicted (HOFFMAN and DODSON, 1980). The flux is roughly 10^{12} ions m^{-2} s^{-1} within the polar cap for summer and equinox conditions. During the winter the flows are no longer constant across the polar cap and the mean flow is smaller by a factor of about two.

Figure 8 shows that mean values of $|\phi/\phi_L|$, at high latitudes, are larger in winter by a factor of about two. Upward flows raise the ion transition height, giving a proton flux approximately equal to ϕ for steady state conditions. Hence these observations indicate that the limiting O^+ flux in the polar ionosphere, ϕ_L, has similar values in summer and equinox but decreases by a factor of about four in winter. This change would be caused primarily by a similar decrease in O^+ densities in the topside F-region.

Figure 12 shows smoothed contours of (ϕ/ϕ_L) for winter in the northern polar regions. The shaded area denotes the extent of the statistical auroral oval predicted for the mean K_p of the observations. Polynomial fits to Feldstein's ovals by HOLZWORTH and MENG (1975) were employed. The largest values of (ϕ/ϕ_L) were obtained within the polar cap in the post-midnight sector. This maximum broadly coincides with the polar 'hole' depletion of the F-layer, as observed at 300 km by BRINTON *et al.* (1978) using winter data from the AE-C ion mass spectrometer. The hole has been modelled for these conditions by SOJKA *et al.* (1981), using a time-dependent, three-dimensional model of the high latitude F-region and including the effects of convective motions. The extent and position of the hole were shown to vary with universal time. Its effects

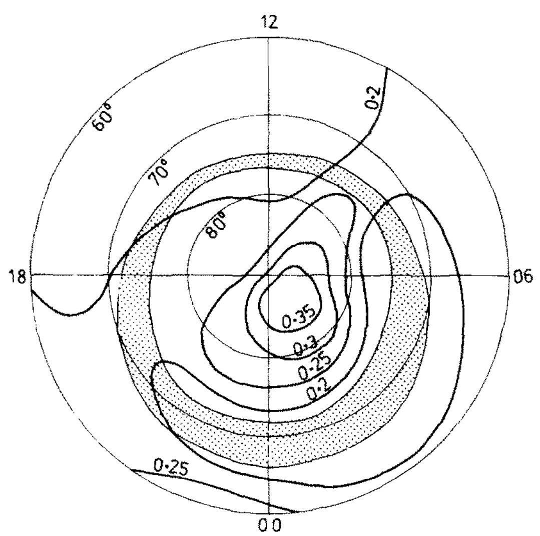

Fig. 12. Geomagnetic latitude—local time plot of contours of (ϕ/ϕ_L) from all observations taken within 50 days of the December solstices over the northern polar regions.

would therefore be smoothed over a large area in Fig. 12, which is an average over all universal time. Mean values of (ϕ/ϕ_L) over the polar cap do show a strong universal time dependence, with a peak at 15 h for the northern hemisphere.

Mean values of proton flow observed by the ISIS 2 mass spectrometer (HOFFMAN and DODSON, 1980) show the flux at 1400 km has a minima in winter, coincident with the minima in the O^+ density, along the 08–20 MLT orbit. The depression observed near the pole may be the sunward edge of the polar hole, as modelled by SOJKA *et al.* (1981); across this the proton flow decreases by a factor of approximately five. The O^+ depletion at 1400 km is a factor of about ten, as is observed for the hole at 300 km (BRINTON *et al.*, 1978) and is modelled by SOJKA *et al.* (1981). The limiting O^+ flux is proportional to the O^+ density [equation (6)] and hence, if neutral density and temperature are constant across the hole, it too is reduced by about ten. Together these observations require that if the O^+ flow is approximately equal to the H^+ flow it supports, then (ϕ/ϕ_L) is enhanced by a factor of two within the hole. This is consistent with Fig. 12.

Figure 8 has persistent minima at latitudes of about 65°, near the auroral oval and the poleward edge of the mid-latitude trough. Figure 12 shows that this minimum extends from about 20.00 LT to 09.00 LT during winter. The polar wind outflow of light ions still occurs on these closed field lines outside the plasmapause and often penetrates to within the plasmasphere (TITHERIDGE, 1976c). The ISIS 2 observations in winter reveal a small reduction of proton flux between the polar cap and the plasmapause in the dawn sector (HOFFMAN and DODSON, 1980). This reduction is at most a factor of two, which can make only a partial contribution to the minima in (ϕ/ϕ_L). Furthermore it is absent entirely from the summer and equinox data, when minima in (ϕ/ϕ_L) are still observed. Within the auroral torus, F-region densities are increased by low energy particle precipitation. The enhancement modelled by SOJKA *et al.* (1981) is sufficient to explain the minima through the increase of ϕ_L alone.

An additional factor which could affect the values of (ϕ/ϕ_L) deduced at auroral latitudes is a departure from steady state, due to rapid changes in horizontal motion. Plasma which has convected over the polar cap is moved rapidly towards dawn around the auroral oval (e.g. EVANS *et al.*, 1980). To study the effects of this rapid change in convective flow on the plasma density profile, a time-dependent three-dimensional, numerical model was employed by SCHUNK *et al.* (1976). In the cases they modelled the scale-height signature which is calibrated here (Fig. 2) is seen to be altered by the sudden change in convective motion. This effect would be largest in the post-midnight sector but small before midnight, when convective and co-rotational electric fields cancel and horizontal plasma velocities are low (SPIRO *et al.*, 1978). For the example of SCHUNK *et al.* (1976), where upward flow (to support polar wind escape) is included, the contribution to the signature by departures from steady state is much smaller than that due to upward flow. Consequently the major contribution to the minimum in (ϕ/ϕ_L) is expected to be enhanced ion density within the auroral torus. Around 09.00 LT plasma convects into the sunlit hemisphere for many of the observations used in Fig. 12 which are furthest removed from the winter solstice. The transient response to layer sunrise may then cause a large deviation from steady state and consequently alter (ϕ/ϕ_L). Further features of the high latitude field-aligned O^+ flow are discussed in LOCKWOOD and TITHERIDGE (1981).

6. CONCLUSIONS

Field-aligned fluxes of O^+ in the topside ionosphere (relative to the neutral gas) can be calculated, as a fraction of their limiting value, from topside soundings. The overall accuracy of the deduced value is limited by the accuracy of the observed profile at altitudes well below the satellite and by the necessary use of a model value for the neutral temperature. Upward O^+ flows can be measured more accurately than downward ones and are more closely related to the H^+ flows occurring at greater altitudes. An analysis was made of 10,000 mean electron-density profiles, obtained from *Alouette 1* data at latitudes of 90°N–70°S near the sunspot minimum. Thirty-seven per cent of the profiles show the presence of an appreciable O^+ flux. Calculated values of the flux, ϕ, range up to 60% of the limiting value ϕ_L. The errors in ϕ are typically a few per cent of ϕ_L. Since the direction of flow is not readily determined, results are presented as mean values of $|\phi/\phi_L|$.

The O^+ fluxes are largest at geomagnetic latitudes of less than about 20°, in the region of the equatorial fountain. The corresponding field lines are below the protonosphere at all points and there are large inter-hemispheric flows. Calculated mean fluxes have a sharp minimum at 06.00 LT when plasma densities are least. Mean values of $|\phi/\phi_L|$ in the equatorial zone, averaged over all local times, are about 0.22 for equinox conditions and 0.25 near the solstices.

At mid-latitudes, changing O^+ flows reflect the diurnal cycle of protonospheric replenishment. Mean values of $|\phi/\phi_L|$ over the range 30–50° geomagnetic latitude are about 0.1 in summer and 0.06 in winter. Mean equinoctial values are 0.08 for the northern hemisphere and 0.13 for the southern. Near the September equinox the flux ratio, averaged over all local times, is 70% greater in the southern hemisphere than in the northern hemisphere.

Refilling of the protonosphere, after large magnetic storms, is shown by an increase in $|\phi/\phi_L|$. This increase persists for about 4 days after the sudden commencement, at latitudes of 10–30°. At mid-latitudes (30–50°) flux ratios are enhanced for about 7 days, and the normal diurnal variation is not re-established for about 10 days after a large sudden-commencement storm.

At high latitudes the outflow of light ions is relatively constant and upwards and the departures from diffusive equilibrium required to support the polar wind tend to reflect variations in the limiting O^+ flux. Thus at latitudes near 65°, ϕ/ϕ_L is decreased between about 20.00 and 09.00 LT in winter. The decrease is in agreement with calculated increases in O^+ densities in the auroral zone, which cause an increase in ϕ_L. At polar latitudes the ratio ϕ/ϕ_L is largest in winter. This arises from a decrease in ϕ_L, as the density of the topside ionosphere decreases.

Acknowledgements—Initial research for this work was carried out at the Communications Research Centre, Ottawa, Canada. One of the authors (M.L.) thanks the Council of the University of Auckland for the award of a Post-Doctoral Research Fellowship. The authors are grateful to Dr. H. RISHBETH for valuable discussion, to the staff of the Radio Research Centre and Mrs M. G. HUDSPITH for the preparation of this manuscript.

REFERENCES

BAILEY G. J. and MOFFETT R. J. 1979 *Planet. Space Sci.* **27**, 1075.
BAILEY G. J., MOFFETT R. J. and MURPHY J. A. 1977a *Planet. Space Sci.* **25**, 967.
BAILEY G. J., MOFFETT R. J. and MURPHY J. A. 1977b *J. atmos. terr. Phys.* **39**, 105.
BAILEY G. J., MOFFETT R. J. and MURPHY J. A. 1978 *Planet. Space Sci.* **26**, 753.
BANKS P. M. and HOLZER T. E. 1969a *J. geophys. Res.* **26**, 6304.
BANKS P. M. and HOLZER T. E. 1969b *J. geophys. Res.* **26**, 6317.
BANKS P. M. and KOCKARTS G. 1973 *Aeronomy*, Part B, Academic Press, New York.
BRINTON H. C., GREBOWSKY J. M. and BRACE L. H. 1978 *J. geophys. Res.* **83**, 4767.
EVANS J. V. 1975 *Planet. Space Sci.* **23**, 1461.
EVANS J. V. and HOLT J. M. 1978 *Planet. Space Sci.* **26**, 727.

EVANS J. V., HOLT J. M., OLIVER W. L. and WAND R. H. 1980 *J. geophys. Res.* **85**, 41.
GEISLER J. E. 1967 *J. geophys. Res.* **72**, 81.
HANSON W. B. and PATTERSON T. N. L. 1964 *Planet. Space Sci.* **12**, 979.
HEDIN A. E., SALAH J. E., EVANS J. V., REBER C. A., NEWTON, G. P., SPENCER N. W., KAYSER D. C., ALCAYDE D., BAUER P., COGGER L. and MCCLURE J. P. 1977 *J. geophys. Res.* **82**, 2139.
HEELIS R. A., BAILEY G. J. and HANSON W. B. 1978 *J. geophys. Res.* **83**, 3683.
HOFFMAN J. H. and DODSON W. H. 1980 *J. geophys. Res.* **85**, 626.
HOLZWORTH R. H. and MENG C. I. 1975 *Geophys. Res. Lett.* **2**, 377.
LOCKWOOD M. and TITHERIDGE J. E. 1981 *Geophys. Res. Lett.* **8**, 381.
MARUBASHI K. 1979 *Planet. Space Sci.* **27**, 603.
MURPHY J. A., BAILEY G. J. and MOFFETT R. J. 1976 *J. atmos. terr. Phys.* **38**, 351.
PARK C. G. 1974 *J. geophys. Res.* **79**, 169.
RAITT W. J. and DORLING E. B. 1976 *J. atmos. terr. Phys.* **38**, 1077.
RAJARAM G. 1977 *J. atmos. terr. Phys.* **39**, 1125.
RISHBETH H. 1977 *J. atmos. terr. Phys.* **39**, 1159.
RISHBETH H., VAN ZANDT T. E. and HANSON W. B. 1977 *Planet. Space Sci.* **25**, 629.
SCHUNK R. W., BANKS P. M. and RAITT W. J. 1976 *J. geophys. Res.* **81**, 3271.
SOJKA J. J., RAITT W. J. and SCHUNK R. W. 1981 *J. geophys. Res.* **86**, 2206.
SPIRO R. W., HEELIS R. A. and HANSON W. B. 1978 *J. geophys. Res.* **83**, 4255.
TITHERIDGE J. E. 1968 *J. atmos. terr. Phys.* **30**, 1843.
TITHERIDGE J. E. 1973 *Planet. Space Sci.* **21**, 1775.
TITHERIDGE J. E. 1976a *Planet. Space Sci.* **24**, 229.
TITHERIDGE J. E. 1976b *Planet. Space Sci.* **24**, 247.
TITHERIDGE J. E. 1976c *J. geophys. Res.* **81**, 3227.
VICKREY J. F., SWARTZ W. E. and FARLEY D. T. 1979 *J. geophys. Res.* **84**, 7307.
YOUNG E. R., TORR D. G., RICHARDS P. and NAGY A. F. 1980 *Planet. Space Sci.* **28**, 881.

APPENDIX A. FACTORS WHICH INFLUENCE (ϕ/ϕ_L)

Consider a Cartesian coordinate system with the z-axis aligned with ∇N_i and the x-direction defined such that the geomagnetic field, **B**, lies in the zx-plane and makes an angle α with the x-axis. (If the plasma is horizontally stratified z is vertically upward, x is horizontally southward and α equals the magnetic dip, I.) In a direction k, let the ion and neutral velocities be v_k and u_k respectively and let the electric field be E_k. Equations by BANKS and KOCKARTS (1973, Chapter 19) give the ion velocity components when the following assumptions are valid: ions carry a single positive charge; negative charges are electrons; nett charge neutrality of plasma; ion–ion collisions are negligible, steady state conditions.

At F-region heights at all latitudes more than 10° from the geomagnetic equator the ion-neutral collision frequency obeys the inequality

$$\nu_{in}^2 \ll \Omega_i \sin^2 I, \tag{A1}$$

where Ω_i is the ion gyrofrequency. Horizontal plasma gradients are smaller than vertical ones, so $\sin I \simeq \sin\alpha$ and

$$\nu_{in}^2 \ll \Omega_i \sin^2 \alpha, \tag{A2}$$

is taken to apply at middle and high latitudes. Under these conditions

$$v_x = -v_z \cot\alpha - \frac{cE_y}{B\sin\alpha} - \frac{u_y \nu_{in}}{\Omega_i \sin\alpha}, \tag{A3}$$

$$v_z = -v_d - \frac{cE_y \cos\alpha}{B} - \frac{\nu_{in} u_y \cos\alpha}{\Omega_i} + u_z \sin^2\alpha - u_x \sin\alpha\cos\alpha, \tag{A4}$$

where v_d is the diffusion velocity due to the gradient ∇N_i. The value of the field-aligned component of a vector **a** is given by

$$a_{II} = a_x \cos\alpha - a_z \sin\alpha, \tag{A5}$$

hence from equations (A3), (A4) and (A5)

$$v_{II} \sim \frac{v_d}{\sin\alpha} + u_x \cos\alpha - u_z \sin\alpha. \tag{A6}$$

From equation (A5) and the definition of ϕ given in equation (5) of the text

$$\phi = N_i(v_{II} - u_{II}) = \frac{N_i v_d}{\sin\alpha}. \tag{A7}$$

APPENDIX B. EFFECT OF ION-INERTIAL TERMS

Inclusion of ion-inertial terms in equation (2) of the text gives

$$\phi = \phi' - \frac{N_i m_i}{DN_n}\left[\frac{dv_{II}}{dt} + v_{II}\sin I\left(\frac{dv_{II}}{dh}\right)\right], \tag{B1}$$

where ϕ' is the value of the flux determined by neglecting ion-inertial effects. Under steady state conditions and in the absence of production or loss of ions the continuity equation reduces to

$$\frac{\mathrm{d}}{\mathrm{d}h}(N_i v_{ii}) = N_i \frac{\mathrm{d}v_{ii}}{\mathrm{d}h} - \frac{v_{ii} N_i}{H} = 0. \tag{B2}$$

From equations (B1), (B2) and (6) of text

$$\phi = \phi'\left(1 - \frac{v_{ii}^2}{gx}\right), \tag{B3}$$

where

$$x = (H_0 - H)\left[\frac{k}{m_i g}\left(\frac{\mathrm{d}T_i}{\mathrm{d}h}\right) + 1\right]. \tag{B4}$$

Applying equation (B3) to the limiting flux conditions (when $v_{ii} = v_L$, $x = x_L$ and $H = H_n$) gives ε, the fractional error in (ϕ/ϕ_L) caused by neglect of ion-inertial effects, as

$$\varepsilon \simeq \left\{\frac{v_L^2}{gx_L} - \frac{v_{ii}^2}{gx}\right\} \Bigg/ \left\{1 - \frac{v_{ii}^2}{gx}\right\}. \tag{B5}$$

If the field-aligned ion velocities are mainly due to diffusion then the term in equation (B5) due to ϕ_L dominates and the value of v_L which causes an error ε is

$$v_L \simeq (g\varepsilon x_L)^{1/2}. \tag{B6}$$

To cause a 5% error in (ϕ/ϕ_L), which is comparable to the other errors, the diffusion velocity at the height h_d must exceed about 250 m s^{-1} under limiting flux conditions. The flux ratio is always underestimated by the amount of this error.

If the field-aligned velocities contain a larger component due to thermospheric motions (particularly meridional horizontal winds at lower latitudes) the errors in ϕ and ϕ_L become comparable and by equation (B5) the error in (ϕ/ϕ_L) is reduced.